Hybrid Materials

DOI: 10.1002/ange.200906977

Substrate Size-Selective Catalysis with Zeolite-Encapsulated Gold Nanoparticles**

Anders B. Laursen, Karen T. Højholt, Lars F. Lundegaard, Søren B. Simonsen, Stig Helveg, Ferdi Schüth, Michael Paul, Jan-Dierk Grunwaldt, Søren Kegnæs, Claus H. Christensen, and Kresten Egeblad**

Over the years, many strategies have been developed to address the problem of sintering of nanoparticle catalysts,[1] including encapsulating metal nanoparticles in protective shells,[2–4] and trapping nanoparticles in the cavities of certain zeolites in post-synthesis steps.[5–8] In general, materials that contain metal nanoparticles that are only accessible via zeolite micropores are intriguing, specifically, but not exclusively, for catalytic applications. The encapsulation of carbon nanoparticles during zeolite crystallization is a well-known approach for making carbon–zeolite composites that afford mesoporous zeolites after combustion.[9–11] Herein, we show that metal nanoparticles can also be encapsulated during zeolite crystallization, as exemplified by silicalite-1 crystals that are embedded with circa 1–2 nm-sized gold nanoparticles that remain stable and catalytically active after calcination in air at 550 °C. Moreover, we show that the encapsulated gold nanoparticles are only are accessible through the micropores of the zeolite, which makes this material a substrate-size selective oxidation catalyst.

Currently, more than 175 different zeolite structures have been reported,[12] and these can be tuned according to the desired acidity and/or redox properties. Expanding the scope from pure zeolites to hybrid materials, by combining the properties of zeolites with other components, significantly widens the field of zeolite materials design. Aside from post-treatment methods, two types of approaches have been pursued for preparing hybrid zeolite–nanoparticle materials. The first type of approach involves crystallization of the zeolite from a gel that contains metal ions that are immobilized in the zeolite during crystallization.[13–14] With this kind of approach, it is very difficult to control the properties of the non-zeolite component in terms of, for example, particle size. The other type of approach is to first synthesize the non-zeolite component and subsequently encapsulate this in the individual zeolite crystals during crystallization. Indeed, this strategy is also well-known and an entire family of materials, known as mesoporous or hierarchical zeolite crystals, are based on the embedding of carbon nanoparticles, nanofibers, nanotubes, or other nanostructures during zeolite crystallization (and subsequent combustion) in a process known as carbon templating.[9–11,15,16] Concerning the embedding of metal nanoparticles in zeolites, Hashimoto et al. reported a top down approach that features downsizing gold flakes to approximately 40 nm particles by laser ablation, and subsequent encapsulation of these particles during crystallization.[17] A reduction in particle size by one order of magnitude is necessary for an efficient use of costly noble metals in catalytic applications. However, a reduction of the particle size enhances the tendency for sintering, owing to the increase in surface free energy. To mitigate this problem, we report herein a bottom-up approach for the preparation of hybrid zeolite-nanoparticle materials that contain small metal nanoparticles, dispersed throughout the zeolite crystals. This synthetic approach comprises three steps (Figure 1): First, a metal nanoparticle colloid is prepared with suitable anchor points for the generation of a silica shell. Second, the particles are encapsulated in an amorphous silica matrix. Third, the silica nanoparticle precursor is subjected to hydrothermal conditions in order for zeolite crystallization to take place. Using this approach, we successfully prepared a material that consisted predominantly of circa 1–2 nm sized gold particles that were embedded in silicalite-1 crystals. X-ray diffraction revealed that the material contained exclusively gold as well as MFI-structured material (generalized silicalite-1 crystal structure type).

Figure 2 shows scanning electron microscopy (SEM) and transmission electron microscopy (TEM) images of the hybrid material that consists of gold nanoparticles embedded in silicalite-1 crystals. The SEM image reveals that the material is mainly composed of circa 1–2 μm long coffin-shaped crystals, with a minor fraction of intergrown coffin-

[*] A. B. Laursen, K. T. Højholt, L. F. Lundegaard, S. B. Simonsen, S. Helveg, Prof. C. H. Christensen, K. Egeblad
Haldor Topsøe A/S
Nymøllevej 55, 2800 Kgs. Lyngby (Denmark)
E-mail: chc@topsoe.dk
kreg@topsoe.dk

A. B. Laursen, Prof. J.-D. Grunwaldt
DTU Chemical Engineering
Technical University of Denmark
2800 Kgs. Lyngby (Denmark)

K. T. Højholt, S. Kegnæs, Prof. C. H. Christensen, K. Egeblad
Center for Sustainable and Green Chemistry
Technical University of Denmark
2800 Kgs. Lyngby (Denmark)

Prof. Dr. F. Schüth, M. Paul
Max-Planck-Institut für Kohlenforschung
45470 Mülheim (Germany)

[**] We gratefully acknowledge the participation of the CTCI Foundation, Taiwan, in the establishment of the in situ electron microscopy facility at Haldor Topsøe A/S and the Catalysis for Sustainable Energy Initiative, Technical University of Denmark.

Supporting information for this article, including experimental procedures and TEM movies, is available on the WWW under http://dx.doi.org/10.1002/anie.200906977.

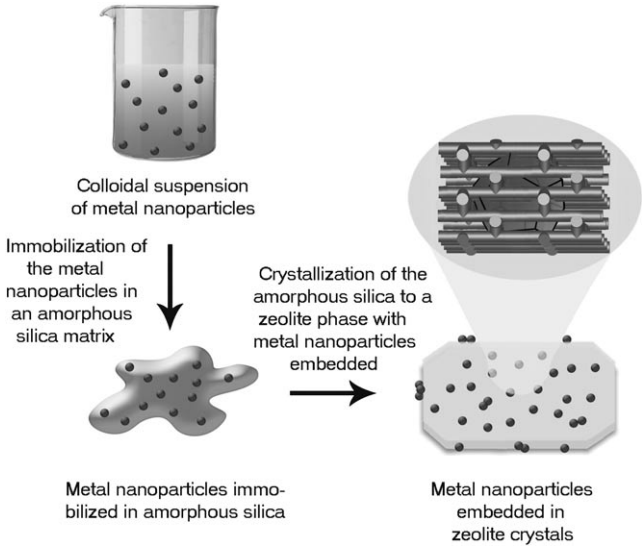

Figure 1. Schematic illustration of the encapsulation of gold nanoparticles in zeolite crystals.

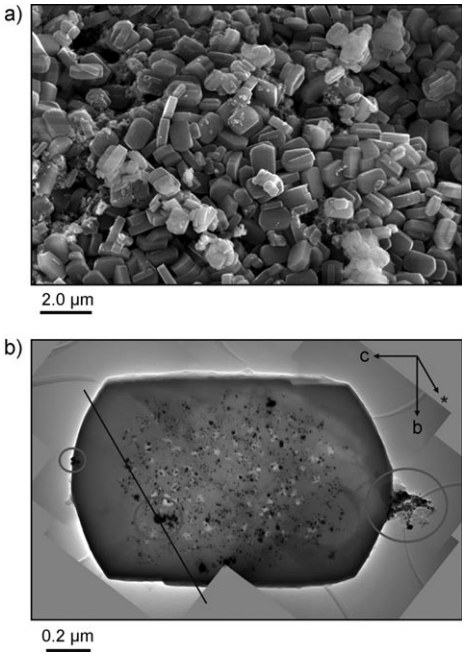

Figure 2. SEM and TEM micrographs of the composite zeolite sample. a) SEM micrograph showing the coffin-shaped crystallites, characteristic for silicalite-1. b) Mosaic composed of 10 TEM bright-field micrographs that shows a representative crystallite as seen along the [1 0 0] zone axis. The crystal lattice is indexed based on the standard *Pnma* space group setting. The black areas represent high density regions, and therefore correspond to the gold particles. Voids are observed as light regions within the zeolite crystal. Circles mark gold particles that are either obviously on the surfaces or are later shown to be on the surface of the crystallite (cf. Figure 3).

shaped crystals and irregularly shaped crystals (Figure 2a). The coffin-shaped and intergrown coffin-shaped crystal morphologies are commonly observed for MFI-structured zeolite materials. The mosaic TEM image reveals an overall uniform contrast over the entire crystal, superimposed by areas of darker and brighter contrast (Figure 2b). The variable contrast is attributed to variable mass-thickness over the crystal: the darker areas correspond to gold particles and the brighter areas correspond to voids in the crystal. The very small voids are consistent with small mesoporosity, measured by N_2 physisorption (see the Supporting Information). Gold particles that are observed in plan view in the crystal are approximately 1–2 nm in diameter, whereas those imaged in the profile view at the crystal edges are significantly larger and more agglomerated. The voids appear to be concentrated in the center of the crystal, around the gold particles. Similar observations, that the formation of metal nanoparticles induce secondary pore formation in zeolites, have been reported previously, for instance for platinum nanoparticles in zeolite NaX.[18] As a TEM image is a two-dimensional projection of the specimen, it is not possible to determine whether the small particles are located on the crystal surfaces or inside the zeolite crystal. To determine the relative positions of the gold nanocrystals with respect to the zeolite crystal, three-dimensional imaging was pursued by means of bright field TEM tomography.[19–21]

The reconstructed tomogram shows all of the characteristic features that were observed in the TEM images apart from the smallest gold particles; this is a result of the blurring effect caused by the weighted back-projection algorithm. From the tomogram sections, shown in Figure 3, it is clear that significant amounts of gold are located inside the zeolite crystal. Investigation of all of the tomogram sections shows that all of the gold particles shown in Figure 2b (except those marked by the circles) are encapsulated within the zeolite crystal.

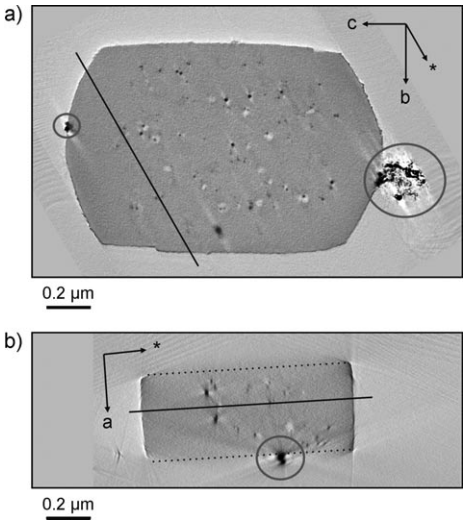

Figure 3. Sections through tomogram reconstruction. Images in a) and b) are tomogram sections approximately perpendicular to and parallel to the [1 0 0] zone axis, respectively. The full lines in each section correspond to the intersection of the other tomogram section. The missing wedge of the tilt series parallel to the [1 0 0] zone axis results in low contrast on crystal surfaces normal to this direction. Dotted lines have been added to clearly show the position of the {1 0 0} surfaces in b). Red circles mark gold particles on the surface of the zeolite crystal (compare to Figure 2).

To address if the zeolite encapsulation stabilizes the gold nanocrystals, TEM images were recorded before and after calcination (550 °C in air, 3 hours; Figure 4a,b). Before calcination, the majority of the gold particles were generally circa 1 nm in diameter (Figure 4a). However, after calcination, the particles imaged in profile view at the edges are larger and more rounded in shape (Figure 4b), whereas the majority of the particles imaged in the plane view in the crystal remain unaltered in size. This observation indicates that the gold particles that are embedded within the zeolite crystals have an enhanced stability towards sintering, despite the smaller gold particle size. Therefore, this synthesis affords a gold–silicalite-1 hybrid material with an enhanced sintering stability of the metal nanoparticles.

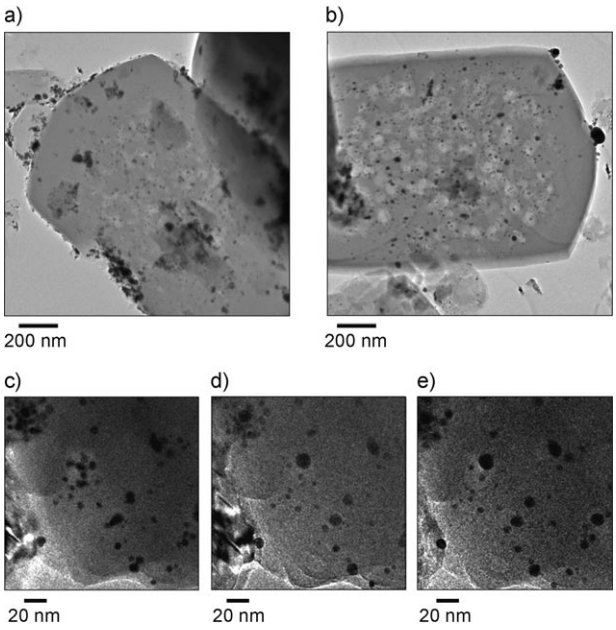

Figure 4. TEM images a) before and b) after calcination (550 °C, 3 h). In situ TEM images obtained under an O_2 atmosphere at c) 25, d) 300, and e) 500 °C.

The enhanced stabilization of the gold nanoparticles is further corroborated by a series of in situ TEM images (Figure 4c–e) that were obtained during exposure of the material to an O_2 atmosphere at temperatures from 25–500 °C. At 25 °C, the sample area contains gold particles of different sizes (Figure 4c). By heating to 300 °C, and further up to 500 °C, the larger gold particles preferentially sinter whilst the smallest particles are stable. This could be regarded as unexpected, as the sintering rate of nanoparticles usually scales inversely with their size. However, in this material, the small nanoparticles are less prone to sintering because they are fixed within the zeolite crystal. Given the information obtained from Figure 4a–b, the in situ observation is fully consistent with the finding that particle embedment in the zeolite improves their stability towards sintering.

In order to verify that the encapsulated gold nanoparticles are accessible for catalysis, we investigated the aerobic oxidation of a mixture of benzaldehyde and 3,5-di-*tert*-butylbenzaldehyde in methanol into their corresponding methyl esters. The reaction was conducted at room temperature under atmospheric pressure.[22,23] The results of these experiments, together with reference experiments carried out using a Au/TiO_2 catalyst, are shown in Figure 5. Both substrates are oxidized using the Au/TiO_2 catalyst, whereas only benzaldehyde is oxidized in appreciable amounts using the gold–silicalite-1 catalyst. This observation is attributed to the different size of the substrates; 3,5-di-*tert*-butylbenzaldehyde is much more bulky than the unsubstituted benzaldehyde, and is therefore not able to diffuse into the zeolite interior where the catalytically active gold nanoparticles are located.

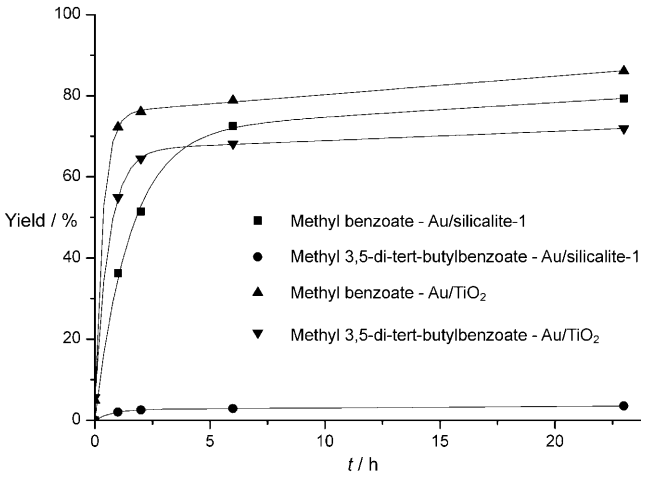

Figure 5. Gold-catalyzed oxidation of a mixture of benzaldehyde and 3,5-di-*tert*-butylbenzaldehyde in methanol to form the methyl esters.

In summary, we have developed an approach for the preparation of hybrid materials that are comprised of 1–2 nm sized gold nanoparticles that are embedded in silicalite-1 crystals. We have shown by three-dimensional TEM tomography that some gold particles are embedded within the zeolite and some are on the external surface of the zeolite crystals. Moreover, calcination experiments, followed by both ex situ and in situ TEM, indicate that the nanoparticles embedded within the zeolite crystals are highly stable towards sintering, whereas the particles located on the outer surface of the zeolite tend to sinter. Furthermore, we have shown that the encapsulated gold nanoparticles are only accessible through the zeolite micropores as it is not possible to oxidize 3,5-di-*tert*-butylbenzaldehyde whereas benzaldehyde is readily oxidized. Therefore, hybrid materials such as these might find application as sinter-stable nanoparticle catalysts or in other areas of materials science.

Received: December 11, 2009
Revised: January 19, 2010
Published online: April 9, 2010

Keywords: gold · mesoporous materials · nanoparticles · oxidation · zeolites

[1] C. H. Christensen, J. K. Nørskov, *Science* **2010**, *327*, 278 – 279.
[2] P. M. Arnal, M. Comotti, F. Schüth, *Angew. Chem.* **2006**, *118*, 8404 – 8407; *Angew. Chem. Int. Ed.* **2006**, *45*, 8224 – 8227.
[3] S. H. Joo, J. Y. Park, C.-K. Tsung, Y. Yamada, P. Yang, G. A. Somorjai, *Nat. Mater.* **2009**, *8*, 126 – 131.
[4] N. Ren, Y.-H. Yang, J. Shen, Y. Zhang, H.-L. Xu, Z. Gao, Y. Tang, *J. Catal.* **2007**, *251*, 182 – 188.
[5] J. C. Fierro-Gonzalez, Y. Hao, B. C. Gates, *J. Phys. Chem. C* **2007**, *111*, 6645 – 6651.
[6] L. F. Nazar, G. A. Ozin, F. Hugues, J. Godber, D. Rancourt, *Angew. Chem.* **1983**, *95*, 645 – 646; *Angew. Chem. Int. Ed. Engl.* **1983**, *22*, 624 – 625; Supplement: L. F. Nazar, G. A. Ozin, F. Hugues, J. Godber, D. Rancourt, *Angew. Chem.* **1983**, *95*, 898 – 919; *Angew. Chem. Int. Ed. Engl.* **1983**, *22*, 898 – 919.
[7] G. Lu, T. Hoffer, L. Guczi, *Catal. Lett.* **1992**, *14*, 207 – 220.
[8] X. S. Zhao, G. Lu, G. J. Millar, *J. Porous Mater.* **1996**, *3*, 61 – 66.
[9] C. J. H. Jacobsen, C. Madsen, J. Jindrich, I. Schmidt, A. Carlsson, *J. Am. Chem. Soc.* **2000**, *122*, 7116 – 7117.
[10] I. Schmidt, A. Boisen, E. Gustavsson, K. Ståhl, S. Pehrson, S. Dahl, A. Carsson, C. J. H. Jacobsen, *Chem. Mater.* **2001**, *13*, 4416 – 4418.
[11] K. Egeblad, C. H. Christensen, M. Kustova, C. H. Christensen, *Chem. Mater.* **2008**, *20*, 946 – 960.
[12] C. Baerlocher, L. B. McCusker, D. H. Olson, *Atlas of Zeolite Framework Types*, Elsevier, Amsterdam, **2007**.
[13] P. B. Weisz, V. J. Frilette, R. W. Maatman, E. B. Mower, *J. Catal.* **1962**, *1*, 307 – 312.
[14] H. Yang, H. Chen, J. Chen, O. Omotoso, Z. Ring, *J. Catal.* **2006**, *243*, 36 – 42.
[15] Z. Pavlackova, G. Kosova, N. Zilkova, A. Zukal, J. Cejka, *Stud. Surf. Sci. Catal.* **2006**, *162*, 905 – 912.
[16] A. H. Janssen, I. Schmidt, C. J. H. Jacobsen, A. J. Koster, K. P. De Jong, *Microporous Mesoporous Mater.* **2003**, *65*, 69 – 75.
[17] S. Hashimoto, T. Uwada, H. Masuhara, T. Asahi, *J. Phys. Chem. C* **2008**, *112*, 15089 – 15093.
[18] J. Rathousky, A. Zukal, N. Jaeger, G. Schulz-Ekloff, *Nanostruct. Mater.* **1992**, *1*, 355 – 360.
[19] H. Friedrich, P. E. de Jongh, A. R. Verkleij, K. P. De Jong, *Chem. Rev.* **2009**, *109*, 1613 – 1629.
[20] P. A. Midgley in *Handbook of Microscopy for Nanotechnology* (Eds.: N. Yao, L. Z. Wang), Kluwer Academic Publishers, Dordrecht, **2005**, pp. 601 – 628.
[21] P. A. Midgley, R. E. Dunin-Borkowski, *Nat. Mater.* **2009**, *8*, 271 – 280.
[22] C. Marsden, E. Taarning, D. Hansen, L. Johansen, S. K. Klitgaard, K. Egeblad, C. H. Christensen, *Green Chem.* **2008**, *10*, 168 – 170.
[23] S. K. Klitgaard, A. T. DeLaRiva, S. Helveg, R. M. Werchmeister, C. H. Christensen, *Catal. Lett.* **2008**, *126*, 213 – 217.

